

# *In situ* polymerization preparation of blends of poly(methyl methacrylate) and poly(styrene-co-acrylonitrile)

SIXUN ZHENG, JIN LI, QIPENG GUO

*Department of Materials Science and Engineering, University of Science and Technology of China, Hefei 230026, People's Republic of China*

YONGLI MI

*Department of Chemical Engineering, The Hong Kong University of Science and Technology, Clear Water Bay, Kowloon, Hong Kong*

The *in situ* polymerization of methyl methacrylate (MMA) with poly(styrene-co-acrylonitrile) (SAN) was studied. The PMMA/SAN *in situ* polymerization blends obtained were examined by differential scanning calorimetry (DSC), dynamic mechanical analysis (DMA), thermogravimetric analysis (TGA), tensile tests and scanning electron microscopy (SEM). The blends with compositions of 95/5, 80/20, 70/30, and 60/40 in weight ratios were miscible and had a single phase structure. However, the 90/10 PMMA/SAN *in situ* polymerization blend obtained was inhomogeneous and had a two-phase structure; polymerization-induced phase separation occurred during the preparation process of the blend. Both tensile strength and elongation at break increase with increasing SAN content up to 30 wt %. The degradation temperature and thermal stability of PMMA increased remarkably on incorporation of SAN up to 30 wt %.

## 1. Introduction

Polymer blends are becoming more and more important in specific sectors of the polymer industry [1–5], as they can frequently meet performance requirements that cannot be satisfied by the currently available commodity polymers. Consequently, their attractiveness increases with the increasing demands for this class of materials. However, most polymer blend research has focused on materials prepared by conventional mixing of component polymers; the *in situ* formation of polymer blends via the polymerization of a monomer within a polymeric matrix has occasionally been explored [6–15]. The most commercially significant example of *in situ* blend formation is found in the toughening of polymers by rubber modification [6].

It has been known for about 20 years that poly(methyl methacrylate) (PMMA) and poly(styrene-co-acrylonitrile) (SAN), the random copolymers of styrene (S) and acrylonitrile (AN), are miscible [16–19]. PMMA and SAN form a miscible blend over the entire composition range within certain limits of AN content (9–33 wt %) [20,21]. It has been proved that the strong intramolecular repulsive interaction between the S and AN units causes the blend to have a negative enthalpy of mixing [22,23] although no exothermic binary interaction exists between either PMMA and AN or PMMA and S units. The thermodynamic interaction in the blend has been investigated

using small angle neutron scattering (SANS) [24–26], and the phase separation phenomena have been studied above the lower critical solution temperature (LCST) [17, 27]. The kinetics of the development of adhesion at the interface between the two polymers and the diffusion in the blend have also been intensively studied [28–32].

In this work, we report the results of our study on the PMMA/SAN *in situ* polymerization blends. The SAN used had a 25 wt % AN content. The LCST for the blend of PMMA and SAN with 25 wt % AN content was known to be about 250 °C [24]. The blends were prepared by a radical polymerization of methyl methacrylate (MMA) monomer in the presence of SAN. The ceiling temperature of the polymerization reaction was 100 °C, which is much lower than the LCST (250 °C) of the blend. The miscibility, structure, and properties of the PMMA/SAN blends obtained by *in situ* polymerization were investigated by differential scanning calorimetry (DSC), dynamic mechanical analysis (DMA), thermogravimetric analysis (TGA), tensile tests and scanning electron microscopy (SEM).

## 2. Materials and methods

### 2.1. Materials and preparation of samples

The poly(styrene-co-acrylonitrile) (SAN) copolymer used was Kibisan PN-127H AS resin with 25 wt %

AN content, which is a product of Chimei Petrochemicals Co., Inc., Taiwan. It had a melting index of 6.0 g/10 min. The SAN had an intrinsic viscosity  $[\eta] = 0.54 \text{ dl g}^{-1}$  in a butanone solution at 30 °C. To calculate the molecular weight, the Mark–Houwink equation was used

$$[\eta] = KM^\alpha \quad (1)$$

where  $M$  is the viscosity-average molecular weight. The values of  $K$  and  $\alpha$  for SAN with the present composition is  $3.6 \times 10^{-2} \text{ ml g}^{-1}$  and 0.62, respectively [33]. The viscosity-average molecular weight was calculated to be 132 000. The methyl methacrylate (MMA) monomer was reagent grade; it was purchased from Wulian Chemical Factory, Shanghai, China. Before polymerization, MMA was washed with 5 wt % NaOH solution to remove the inhibitor and further dried with anhydrous  $\text{Na}_2\text{SO}_4$ .

Poly(methyl methacrylate) (PMMA) was prepared by a conventional radical process initiated by 0.1 wt % of benzoyl peroxide. Polymerization was carried out by heating MMA and peroxide first at 80 °C to get a critical viscosity level, then the solution obtained was poured into a mould to finish the polymerization process successively at 40 °C for 20 h, 80 °C for 4 h and 100 °C for 4 h. The PMMA sample so obtained had an intrinsic viscosity  $[\eta]$  of  $2.61 \text{ dl g}^{-1}$  in an acetone solution at 25 °C. The values of  $K$  and  $\alpha$  of the Mark–Houwink Equation 1 for PMMA in acetone at 25 °C are  $0.55 \times 10^{-2} \text{ ml g}^{-1}$  and 0.73, respectively [33]. Then the viscosity-average molecular weight of the PMMA sample evaluated from the Mark–Houwink Equation 1 was  $2.6 \times 10^6$ .

The PMMA/SAN blends were prepared starting from the dissolution of SAN in the MMA monomer in a ratios of 95/5, 90/10, 80/20, 70/30 and 60/40 by weight. At this point 0.1 wt % benzoyl peroxide relative to monomer was added with stirring, and the temperature was raised to 80 °C. When the viscosity increased to a critical level, the solution was poured into a mould consisting of two polished glass plates separated by teflon spacers sealed by adhesive tape at the four corners and held together by springs. The mould was kept in an oven successively at 40 °C for 20 h, 80 °C for 4 h and 100 °C for 4 h to complete the polymerization reaction.

## 2.2. Measurements

### 2.2.1. DSC

The calorimetric measurements were made on a Perkin-Elmer DSC-7 differential scanning calorimeter in a dry nitrogen atmosphere. The instrument was calibrated with indium as standard. The sample weight used in the DSC cell was kept in the 8 to 12 mg range. The midpoint of the slope change of the heat capacity plot was taken as the glass transition temperature ( $T_g$ ). A heating rate of  $20 \text{ }^\circ\text{C min}^{-1}$  was used.

### 2.2.2. DMA

Dynamic mechanical measurements were carried out on an Imass Dynastat viscoelastic apparatus in nitro-

gen atmosphere, with temperature scanned from 0 to 160 °C. The frequency used was 5 Hz and heating rate was  $3.0 \text{ }^\circ\text{C min}^{-1}$ . Specimen dimensions were  $6.0 \times 0.4 \times 0.18 \text{ cm}^3$ .

### 2.2.3. TGA

Thermal stability to the blends was assessed with a Du Pont TGA 2950 thermogravimetric analyser (TGA). The sample was first ramped to 50 °C and then heated at  $10 \text{ }^\circ\text{C min}^{-1}$  to 500 °C. Measurements were conducted in air.

### 2.2.4. Tensile tests

Tensile tests were carried out on a Shimadzu DCS-5000 universal testing machine at room temperature according to ASTM D638. Standard dumb-bell specimens with a  $4.0 \times 1.0 \times 0.2 \text{ cm}$  neck were used. Average values were obtained from five to ten successful determinations. Crosshead speed was  $0.5 \text{ cm min}^{-1}$  corresponding to a relative strain rate of  $0.125 \text{ min}^{-1}$ .

### 2.2.5. Morphological observations

To investigate the phase structure of the blends, the specimens were fractured under cryogenic conditions using liquid nitrogen. The fractured surface obtained was etched with methanol. The etched samples were dried to remove the solvent. A Hitachi X-650 scanning electron microscope (SEM) was used for observation. Before observation the surfaces were coated with a thin gold layer of 20 nm thickness.

## 3. Results and discussion

### 3.1. Phase behaviour and morphology

The PMMA/SAN blends in the form of sheets with 2 – 5 mm thickness were prepared by polymerization of MMA in the presence of SAN. The specimens of the PMMA/SAN *in situ* polymerization blends obtained with compositions of 95/5, 80/20, 70/30 and 60/40 in weight ratios were transparent, suggesting that these blends were homogeneous and had a single phase structure. However, the 90/10 PMMA/SAN *in situ* polymerization blend obtained was opaque, implying that the blend had a two-phase structure, and polymerization-induced phase separation occurred. Actually, it was observed that the initially homogeneous, clear solution of 90/10 MMA/SAN mixture became cloudy as the polymerization reaction proceeded.

Fig. 1 shows DSC thermograms for the PMMA/SAN *in situ* polymerization blends. It can be seen from Fig. 1 that all of them exhibit one single  $T_g$  dependent on blend composition. The  $T_g$  values of the blends are indicated in Fig. 1. It should be noted that  $T_g$  decreases with SAN content; this is because  $T_g$  of SAN (106 °C) is lower than that of PMMA (122 °C).  $T_g$  marks the characteristic transition of the amorphous region from a glassy state to a rubbery state of a polymer or blend. It is well known that measurement of  $T_g$  is the most convenient and popular way of investigating the miscibility or immiscibility of pairs of

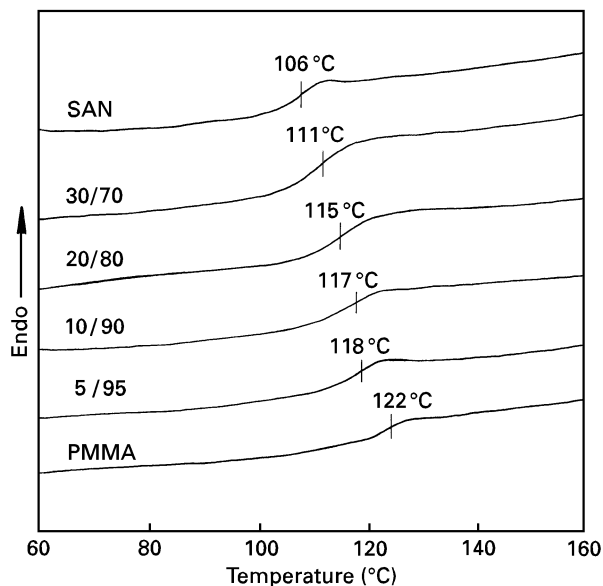


Figure 1 DSC curves for the PMMA/SAN *in situ* polymerization blends.

polymers. In a miscible blend only one  $T_g$  will be observed, whereas two  $T_g$ s will be detected in an immiscible blend. However, the use of  $T_g$  measurements for ascertaining blend miscibility has its limitations. It is difficult to determine the extent of mixing when the difference in the  $T_g$ s of the two polymers is within  $15^\circ\text{C}$ , as the glass transition region usually covers a range of at least  $15^\circ\text{C}$ . In the present case, the difference of the  $T_g$ s of PMMA and SAN is only  $16^\circ\text{C}$ , then it is rather difficult to ascertain the extent of mixing from only the DSC data presented here. However, the occurrence of a single composition-dependent  $T_g$  is in agreement with the conclusion in previous studies [16–19] that PMMA and SAN are miscible.

Fig.2 shows DSC thermograms for a 60/40 PMMA/SAN *in situ* polymerization blend. The blend exhibits a single  $T_g$  of  $79^\circ\text{C}$  as shown in the first scan (curve (a)), which is much lower than that of either PMMA or SAN. The heat capacity overshoot in the first scan (curve(a)) is the result of sub- $T_g$  annealing at the drying temperature. However, the first scan erased the overshoot, and the second scan after heating to  $180^\circ\text{C}$  exhibits a higher  $T_g$  of  $87^\circ\text{C}$  (curve (b)). The remarkable lowering of  $T_g$  observed for the 60/40 PMMA/SAN *in situ* polymerization blend can be considered to be due to insufficient polymerization of MMA. The high viscosity of the 60/40 MMA/SAN mixture greatly retarded the completion of the polymerization reaction. The residual MMA monomer in the blend will greatly reduce the  $T_g$  of the blend.

Fig.3 shows dynamic mechanical spectra of the as-polymerized PMMA as well as the 80/20 and 60/40 PMMA/SAN *in situ* polymerization blends. It can be seen from Fig.3 that the dynamic mechanical spectrum of the as-polymerized PMMA (curve (a)) exhibits a well-defined peak centred at  $139^\circ\text{C}$  on the  $\tan \delta$  versus temperature curve, which is ascribed to its glass transition. The dynamic mechanical spectra of both the 80/20 (curve (b)) and 60/40 (curve (c)) PMMA/

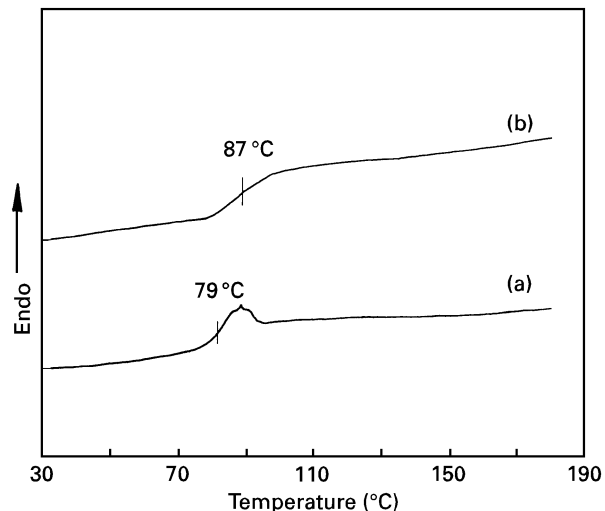


Figure 2 DSC curves for a 60/40 PMMA/SAN *in situ* polymerization blend. (a) First scan; (b) second scan after heating to  $180^\circ\text{C}$ .

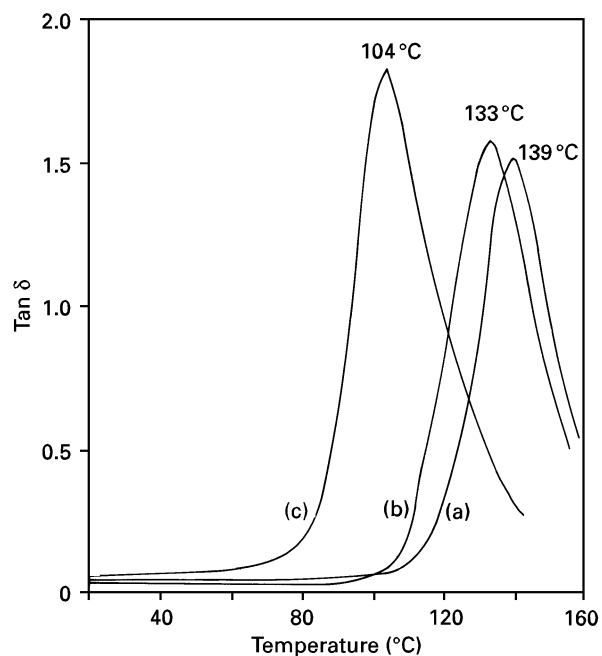


Figure 3 Dynamic mechanical spectra of (a) 100/0, (b) 80/20 and (c) 60/40 PMMA/SAN *in situ* polymerization blends.

SAN *in situ* polymerization blends also display single, sharp peaks, respectively, at  $133$  and  $104^\circ\text{C}$  on the  $\tan \delta$  versus temperature curve, corresponding to the  $T_g$ s of the blends. It is noted that the DMA result presented here further indicates that the 60/40 PMMA/SAN *in situ* polymerization blend had a much lower  $T_g$  value than expected.

The morphology of the PMMA/SAN *in situ* polymerization blends were investigated by means of scanning electron microscopy (SEM). The fractured surfaces of the blend specimens frozen by liquid nitrogen presented no characteristics of a heterogeneous, two-phase blend. Fig. 4 shows the SEM micrographs of methanol-etched fracture surfaces of the blend specimens frozen by liquid nitrogen. It can be seen from Fig.4a that the 90/10 PMMA/SAN blend displays a heterogeneous morphology and there appear to be

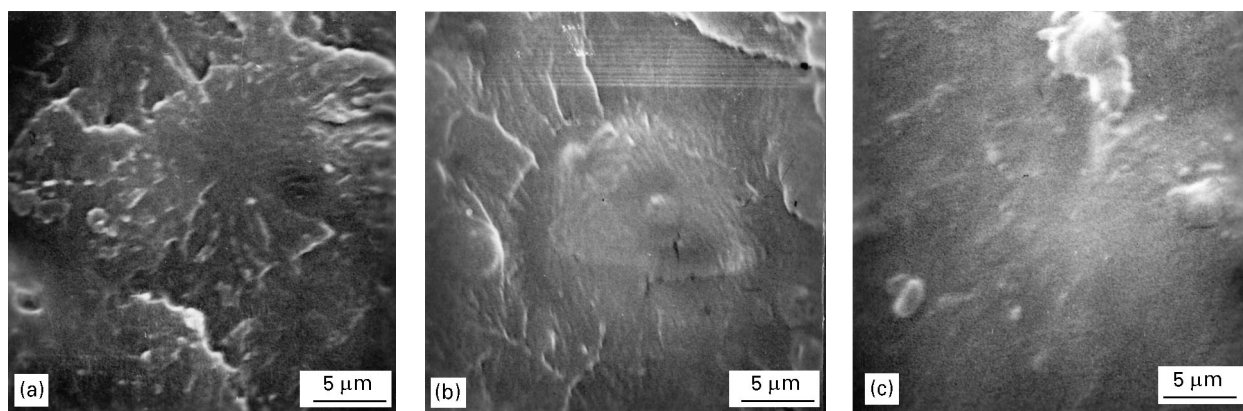


Figure 4 Scanning electron micrographs of the fractured surfaces of the PMMA/SAN *in situ* polymerization blends etched with methanol. Blend composition PMMA/SAN: (a) 90/10, (b) 80/20 and (c) 70/30.

SAN cavities with irregular shapes and broadly-distributed size in diameter after the SAN phase was rinsed out by methanol. It is clear that this blend had a two-phase structure and the dispersions of the minor components are fine. The average domain sizes of the minor SAN phases are smaller than  $0.3\ \mu\text{m}$  in diameter, with the largest of these domains being *c.*  $0.5\ \mu\text{m}$ . However, the SEM micrographs of the etched specimens of the 80/20 (Fig. 4b) and 70/30 (Fig. 4c) blends appear to show no evidence that the blends are heterogeneous.

The results presented here have shown that the PMMA/SAN *in situ* polymerization blends obtained with compositions of 95/5, 80/20, 70/30 and 60/40 weight ratios were miscible and had a single phase structure. However, the 90/10 PMMA/SAN *in situ* polymerization blend obtained was inhomogeneous and had a two-phase structure; polymerization-induced phase separation occurred during the preparation process of the blend.

As shown in the literature, PMMA and SAN with 25 wt % AN content are miscible and the blends show LCST behaviour [16–21, 24]. The LCST for the blend of PMMA and SAN with 25 wt % AN content was known to be about  $250^\circ\text{C}$  [24]. However, in the present case, the 90/10 PMMA/SAN *in situ* polymerization blends had a two-phase structure, as polymerization-induced phase separation occurred. It is noted that the ceiling temperature of the polymerization was only  $100^\circ\text{C}$ , which is rather lower than the phase separation temperature ( $250^\circ\text{C}$ ) of PMMA/SAN blends. PMMA and SAN are miscible at the experimental temperatures, but they rendered immiscible in the presence of MMA as solvent during the *in situ* polymerization preparation of the blends. Solvents are well known to cause heterogeneity in miscible polymer systems [6]. In the present case, the 90/10 inhomogeneous blend was formed when the polymerization route passed through a two-phase region which exists in the MMA/PMMA/SAN three-component phase diagram as shown in Fig. 5. This was proven to be the case. The present result is similar to that for the PMMA/poly(ethylene-co-vinyl acetate) (EVA) *in situ* polymerization blends reported by Chen *et al.* [14]. They investigated the structural develop-

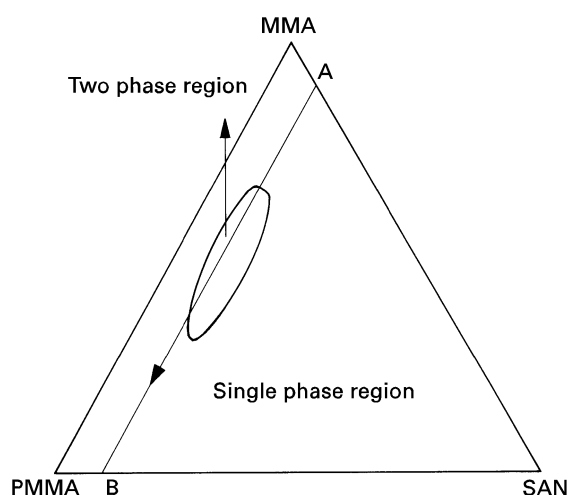


Figure 5 Schematic phase diagram for the MMA/PMMA/SAN system showing an *in situ* polymerization pathway  $A \rightarrow B$  through a two-phase region.

ment during radical polymerization of a mixture of MMA and EVA by light scattering and optical microscopy. It was found that as the polymerization of MMA proceeded, phase separation took place via spinodal decomposition although the mixture of MMA/EVA was initially a single phase.

### 3.2. Tensile properties and thermal stability

The stress–strain curve of the PMMA/SAN *in situ* polymerization blends exhibited brittle fracture characteristics, with no obvious yield observed on the stress–strain curves. This shows that all the blends are basically brittle materials at the strain rate of  $0.125\ \text{min}^{-1}$  and room temperature. From the initial slopes, Young's moduli of the blends were calculated. Table I presents the values of Young's moduli of the blends, together with those of tensile strength and elongation at break. It can be seen that both tensile strength and elongation at break gradually increase with increasing SAN content up to 30 wt %. However, it is noted that the tensile strength and the elongation at break of the 60/40 PMMA/SAN *in situ* polymerization blend was even lower than those of pure

TABLE I Tensile properties of the PMMA/SAN *in situ* polymerization blends

Properties	SAN content (wt %)					
	0	5	10	20	30	40
Tensile modulus (GPa)	2.37	2.33	2.57	3.25	2.67	2.71
Tensile strength (MPa)	63	66	70	71	75	60
Elongation at break (%)	8.4	9.1	10.1	10.5	10.6	7.8

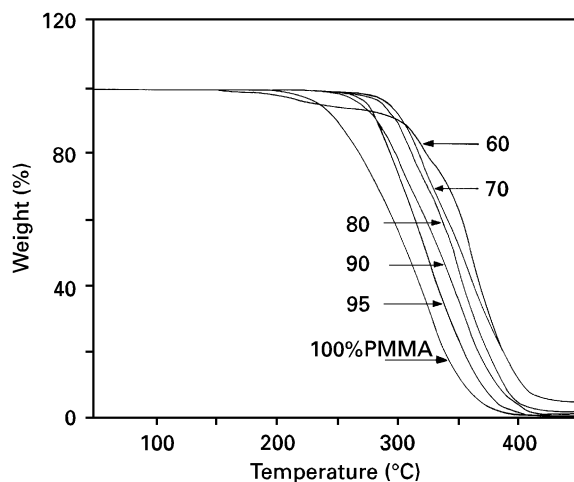


Figure 6 TGA curves for the PMMA/SAN *in situ* polymerization blends heated at  $10^{\circ}\text{C min}^{-1}$  in air.

PMMA. The poor tensile properties of the 60/40 PMMA/SAN *in situ* polymerization blend can be considered to be the result of insufficient polymerization of MMA. This observation is in accordance with the DSC and DMA results.

In order to investigate the thermal stability of the blends, TGA was used to trace the degradation process of the blends in air. Fig. 6 presents TGA curves for the PMMA/SAN *in situ* polymerization blends heated at  $10^{\circ}\text{C min}^{-1}$  in air. It can be seen from Fig. 6 that the onset degradation temperature remarkably increases with increasing SAN content up to 30 wt %. Thermal stability of PMMA was increased by incorporation of SAN up to 30 wt %. It is interesting to see that the 60/40 PMMA/SAN *in situ* polymerization blend exhibited a notable weight loss at temperatures much lower than that at which the pure PMMA and the other blends started to degrade. This can be considered to be due to the insufficient polymerization of MMA in the blend as the high viscosity of the 60/40 MMA/SAN mixture substantially hindered the completion of the polymerization reaction. The weight loss started to occur at much lower temperatures owing to the residual MMA monomer in the 60/40 PMMA/SAN *in situ* polymerization blend. However, it can also be seen from Fig. 6 that the midpoint degradation temperature of the 60/40 PMMA/SAN *in situ* polymerization blend is higher than those of all the other blends, implying that the polymerization of the residual MMA monomer in the blend completed during the heating process of the TGA experiment.

## Acknowledgements

This work was supported by the Presidential Fund of the Chinese Academy of Sciences and by the State Science and Technology Commission of China. One of the authors (Professor Q. P. Guo) wishes to express his appreciation to the State Council of China for granting a National Research Award for Outstanding Young Scientists. Also, the financial support of RGC the Earmarked Grant for Research (No. 581/94E) to this work and to Professor Q. P. Guo for his visit at HKUST is gratefully acknowledged.

## References

1. L. A. ULTRACKI, "Polymer Alloys and Blends" (Hanser Publishers, Munich, 1989).
2. D. R. PAUL and S. NEWMAN (Eds), "Polymer Blends" Vols 1 and 2 (Academic Press, New York, 1978).
3. O. OLABISI, L. M. ROBESON and M. T. SHAW, "Polymer-Polymer Miscibility" (Academic Press, New York 1979).
4. C. B. BUCKNALL, "Toughen Plastics" (Applied Science, London, 1977).
5. A. E. PLATT, in "Comprehensive Polymer Science", edited by G. Allen and J. C. Bevington, (Pergamon, New York, 1989).
6. D. J. WALSH and S. ROSTAMI, *Adv. Polym. Sci.* **70** (1985) 119.
7. D. J. WALSH and J. G. MCKEOWN, *Polymer* **21** (1980) 1330.
8. D. J. WALSH and G. L. CHENG, *ibid.* **23** (1982) 1965.
9. *Idem, ibid.* **25** (1984) 495.
10. L. NELISSEN, E. W. MEIJER and P. J. LEMSTRA, *ibid.* **33** (1992) 3734.
11. U. BERNINI, P. RUSSO, M. MALINCONICO, E. MARTUSCELLI, M. G. VOLPE and P. MORMILE, *J. Mater. Sci.* **28** (1993) 6399.
12. V. DI LIELLO, M. MALINCONICO, E. MARTUSCELLI, G. RAGOSTA, A. RIZZO and M. G. VOLPE, *Angew. Makromol. Chem.* **210** (1993) 47.
13. W. L. NACHLIS, R. P. KAMBOUR and W. J. MACKNIGHT, *Polymer* **35** (1994) 3643.
14. W. J. CHEN, S. KOBAYASHI, T. INOUE, T. OHNAGA and T. OUGIZAWA, *ibid.* **35** (1994) 4015.
15. T. KOJIMA, T. OHNAGA and T. INOUE, *ibid.* **36** (1995) 2197.
16. D. J. STEIN, R. H. JUNG, K. H. ILLERS and H. HENDUS, *Angew. Makromol. Chem.* **36** (1974) 89.
17. L. P. MCMASTER, *Adv. Chem. Ser.* **142** (1975) 43.
18. R. E. BERNSTEIN, C. A. CRUZ, D. R. PAUL and J. W. BARLOW, *Macromolecules* **10** (1977) 681.
19. K. NAITO, G. E. JOHNSON, K. L. ALLARA and T. K. KWEI, *ibid.* **11** (1978) 1260.
20. M. SUESS, J. KRESSLER and H. W. KAMMER, *Polymer* **28** (1987) 957.
21. M. E. FOWLER, J. W. BARLOW and D. R. PAUL, *ibid.* **28** (1987) 2145.
22. J. L. G. PFENNIG, H. KESKKULA, J. W. BARLOW and D. R. PAUL, *Macromolecules* **18** (1985) 1937.
23. M. E. FOWLER, J. W. BARLOW and D. R. PAUL, *Polymer* **28** (1987) 1177.

24. K. HAHN, B. J. SCHMITT, M. KIRSCHHEY, R. G. KIRSTE, H. SALIE and S. SCHMITT-STRECKER, *ibid.* **33** (1992) 5150.
25. J. JELENIC, R. G. KIRSTE, B. J. SCHMITT and S. SCHMITT-STRECKER, *Makromol. Chem.* **180** (1979) 2057.
26. B. J. SCHMITT, R. G. KIRSTE and J. JELENIC, *ibid.* **181** (1980) 1655.
27. J. MARUTA, T. OHNAGA and T. INOUE, *Macromolecules* **26** (1993) 6386.
28. S. YUKIOKA and T. INOUE, *Polym. Commun.* **32** (1991) 17.
29. S. YUKIOKA, K. NAGATO and T. INOUE, *Polymer* **33** (1992) 1171.
30. H. H. KAUSCH and K. JUD, *Plast. Rubber Process. Appl.* **2** (1982) 265.
31. K. JUD, H. H. KAUSCH and J. G. WILLIAMS, *J. Mater. Sci.* **16** (1981) 204.
32. E. KIM, E. J. KRAMER, W. C. WU, and P. D. GARRETT, *Polymer* **35** (1994) 5706.
33. BRANDRUP J. and IMMERGUT E. H. (Eds), "Polymer Handbook", 3rd Edn (John Wiley & Sons Inc., New York, 1989).

*Received 23 February  
and accepted 23 October 1996*